

FIG. 9. Current transients for attachment followed by decay to a secondary ion. Curve 1, primary ion current; curve 2, secondary ion current; curve T, total current.

appropriate limits, the solution is obtained.

$$\rho_2 = \frac{\eta n_0}{[1 + \eta(v_2 - v_1)\lambda]} \times \{ [e^{-\eta(x-v_2t)} - e^{(x-v_2t)/(v_2-v_1)\lambda}] H(x-v_2t) + [e^{(x-v_2t)/(v_2-v_1)\lambda} - e^{-\eta(x-v_1t)} e^{-t/\lambda}] H(x-v_1t) \}. \quad (\text{A16})$$

The currents are obtained by integration in the usual manner.

$$i_1(t) = (v_1 n_0 / a) e^{-t/\lambda} [1 - e^{-\eta(a-v_1t)}] H(a-v_1t), \quad (\text{A17})$$

$$i_2(t) = \frac{v_2 n_0}{a [1 + \eta(v_2 - v_1)\lambda]} \{ [(1 - e^{-\eta(a-v_2t)}) + (v_2 - v_1)\eta\lambda (1 - e^{(a-v_2t)/(v_2-v_1)\lambda})] H(a-v_2t) + [(v_2 - v_1)\eta\lambda (e^{(a-v_2t)/(v_2-v_1)\lambda} - e^{-t/\lambda}) - e^{-t/\lambda} (1 - e^{-\eta(a-v_1t)})] H(a-v_1t) \}. \quad (\text{A18})$$

Illustrations of the shape of these transients are given in Fig. 9. It is interesting to note that if $v_1 < v_2$ there is no break in the current curve, whereas if $v_2 < v_1$ there is a break in the curve at $t = a/v_1$, and the magnitude of the change in slope is $(-\eta v_1^2 n_0 / a) e^{-a/v_1\lambda}$.

Velocity Spectrometer for Mössbauer Experiments*

E. KANKELEIT

California Institute of Technology, Pasadena, California

(Received 23 September 1963; and in final form, 23 October 1963)

An electromechanical feedback system for Mössbauer spectroscopy with a velocity range of 2×10^{-5} to 60 cm/sec is described. A reference signal of the desired waveform (triangle, parabola, etc.) to drive the feedback system is produced by the multichannel analyzer and with the help of operational amplifiers. The linearity of the system for a triangular velocity waveform is better than 0.5% during 98% of the half-period.

INTRODUCTION

WHEN a multichannel analyzer is employed for the velocity spectroscopy in a Mössbauer experiment, two methods are in common use. We shall refer to these two methods as the "modulation mode" and as the "time mode."¹ In the modulation mode a voltage, proportional to the instantaneous velocity, is used to modulate (inside or outside of the analyzer) the detector pulses from a single-channel analyzer in such a way that their pulse height is proportional to the velocity. These pulses are then handled by the analyzer in the ADC mode. The channel number is a linear function of the velocity, provided the analyzer is linear. The CRT of the analyzer then displays a true picture of the velocity spectrum only if, during the meas-

urement, the system spent the same amount of time in each velocity interval. If the velocity of the drive has, for instance, triangular time dependence, i.e., a waveform which increases and decreases linearly in time, this condition is automatically fulfilled, provided that the analyzer deadtime is negligible or constant for all channels. For accurate measurements it is necessary to determine the time spent in a velocity interval. The best way to do this is to run simultaneously a nonresonant spectrum into another part of the memory of the analyzer, which is then taken for normalizing the resonant spectrum.

The main disadvantage of this method is the restriction in the count rate due to the rather long deadtimes involved in addressing each pulse into the memory and the increases of the statistical error of the resonant spectrum by normalizing with the nonresonant spectrum. Even if the first consideration is irrelevant because of low available counting rates, the second contributes to a lengthening of

* Work performed under the auspices of the U. S. Atomic Energy Commission.

¹ Descriptions of these and other methods can be found in H. Frauenfelder, *The Mössbauer Effect* (W. A. Benjamin, Inc., New York, 1962); and A. J. F. Boyle and H. E. Hull, *Rept. Progr. Phys.* **25**, 441 (1962).

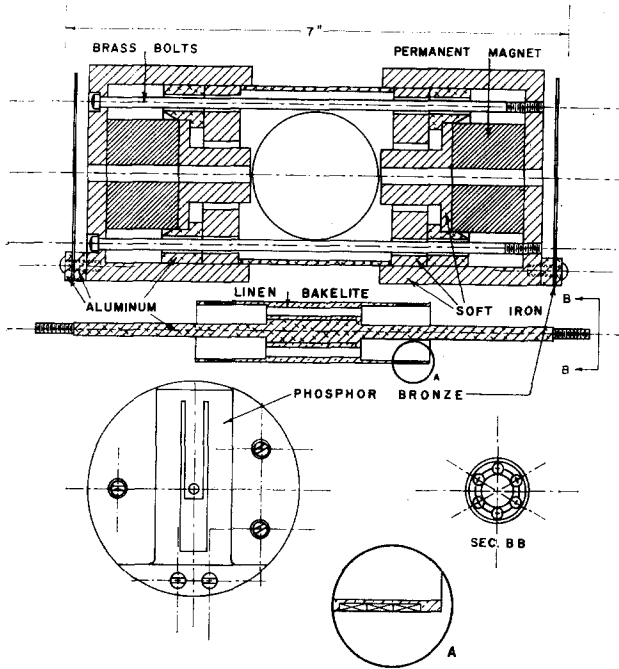


FIG. 2. Details of the electromechanical drive.

loop frequency transfer curve, the importance of which will be mentioned later. The Dana 2200, dc, low noise, wide band amplifier delivers enough amplification and power to drive the system to about 10 cm/sec.

Figure 2 shows the construction of the electromechanical drive. It consists, in principle, of two loudspeaker systems rigidly connected front to front with brass bolts and an aluminum tube as spacer. The permanent magnets (a stock item of Permagan Pacific) produce in the radial air gap a magnetic field of about 5000 G. The field was meas-

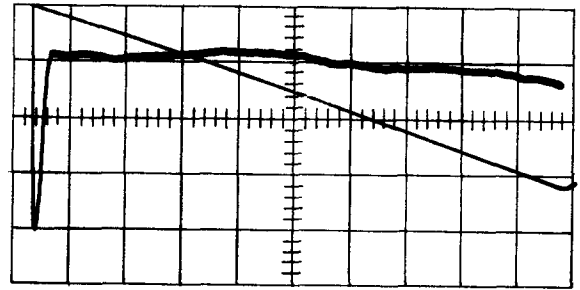


FIG. 3. CRT picture of the half-period of a triangular reference signal and in respect to this a 100-times-amplified error signal.

ured to be constant to less than 0.3% over a length of 0.3 in. in the axial direction. Pickup coil and driving coil are wound in a groove at the ends of one common holder made of linen Bakelite. The coils have a length of 0.3 in. Both coils are subdivided into three coils with a length of 0.1 in. each. The pickup coil consists of three times 350 turns of 0.002-in. wire and the driving coil of 3 times 63 turns of 0.005-in. wire. In the normal operation the three pickup coils are connected in series and the driving coils in parallel. This arrangement allows impedance matching for the driving coil and improvement of the linearity of the pickup coil at very high amplitudes by using only the central coil. The coil holder is pressed and glued onto an aluminum rod. Two phosphor bronze springs, shaped in such a way that the radial displacement is minimal, hold the moving system friction free on the axis.

In addition to the obvious importance of the linearity, the mechanical rigidity of the moving parts in the drive was a point of consideration in the construction of the drive. All drives so far tested show resonance maxima in

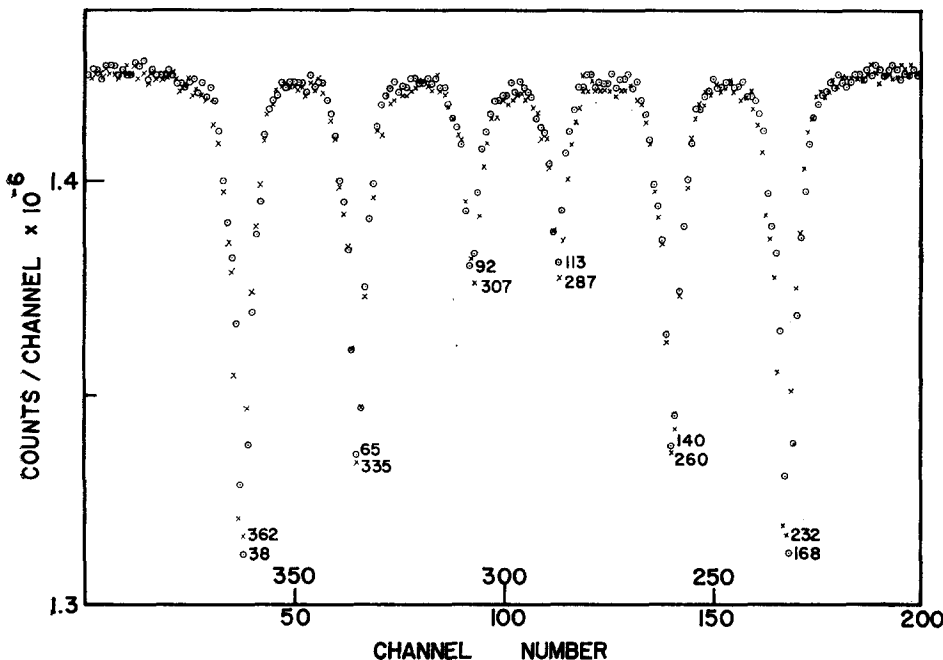
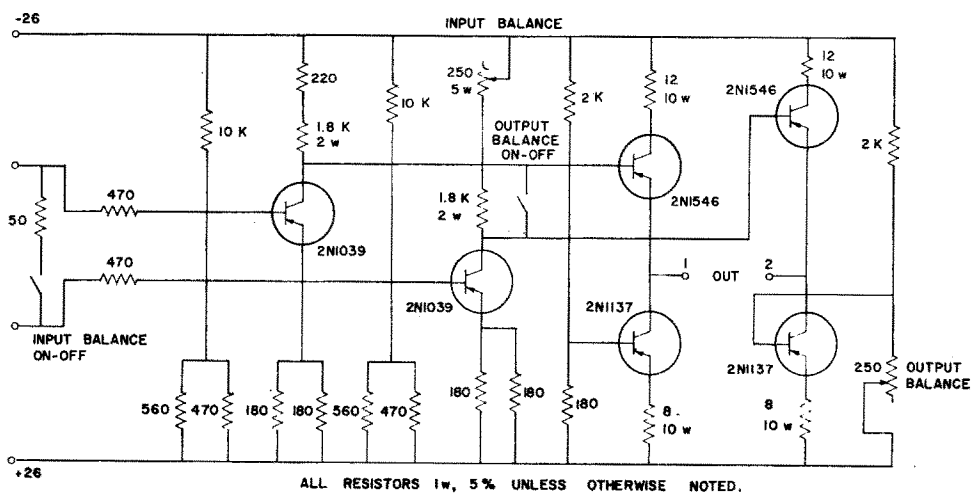


FIG. 4. Velocity spectrum of Fe⁵⁷ with a moved source of Co⁵⁷ diffused into Cu and an Armco iron foil, 0.35 mils thick, as absorber. The channel numbers of the lowest points in the peaks are indicated. Measuring time 700 min.

FIG. 5. Diagram of dc power amplifier.



the frequency transfer curve at several thousand cps. They are due to oscillations in the moving structure of the drive, and they should be eliminated as much as possible. These oscillations, together with the high frequency cutoff of the amplifier, determine the stability range of the feedback system and limit the open loop amplification.

The maximum of the open loop transfer curve lies at the fundamental resonance of the drive. Clearly the fundamental frequency of the reference signal should be close to this resonance to give the best regulation. The highest performance of the system can be achieved by adjusting the above mentioned low-pass filter and the gain at the same time. The optimum setting depends somewhat on the high frequency content of the reference signal. For a sine wave the bandwidth can be reduced and the gain increased. The bandwidth should always be large enough to cancel disturbing influences like sound or small frictions.

The performance of the system is demonstrated in Fig. 3, which shows a CRT picture of a half-period of a triangular reference signal and, in comparison to this, a hundred-times-amplified error signal. The frequency is 25 cps. After a sharp peak of about 1% in amplitude lasting about 2% of the half-period, the deviations are not larger than about 0.1% in amplitude. This picture remains unchanged, also, for higher velocities as long as the amplifier is not driven into saturation.

Figure 4 shows a velocity spectrum of Fe^{57} in an iron foil. As was mentioned above, the spectrum is displayed twice. A first-order distortion in the constancy of the magnetic field in the drive would show up as a shift of one spectrum against the other, especially around zero velocity, i.e., the points of maximum displacement. This is, of course, true only as long as the first half-period is the mirror of the second one. The observable shift of the two curves in Fig. 4 can be attributed to one or both of these effects. The deviations are less than 0.5% of the maximum ve-

locity. Even though it is inconvenient to receive the spectrum twice, it is of great practical advantage to check the quality of the drive system by comparing the two halves. A correction in the velocity scale can easily be performed. In the modulation mode this is not possible and, for instance, the disturbances due to phase shifts of the pickup signal are difficult to recognize.

The drive is capable of moving heavy parts. For experiments on Tm^{169} an oven weighing about 100 g was mounted onto the rod of the drive. The error signal has nearly the same shape as shown in Fig. 3. Only the initial peak becomes larger and broader.

A mechanical drive half the size of that shown in Fig. 2 has been built into a helium cryostat. No difficulties in the operation arose in cooling it down. One only has to correct for the decrease in the resistance of the driving coil by inserting a resistance in series with the coil. A change in calibration of 7% was observed going to liquid nitrogen temperatures.

For velocities above 10 cm/sec the output power of the DANA amplifier is insufficient. A dc power amplifier (Fig. 5) which delivers peak voltages of 40 V into the drive impedance of 60 Ω was constructed. The achievable velocity is about 70 cm/sec. To restrict the amplitudes, higher frequencies are necessary. Heavier springs are then used to increase the resonance frequency of the drive.

The input noise of the DANA amplifier was measured to be about 6 μV rms. With a sensitivity of the pickup coil of 3 cm/sec V the lower limit for the velocity range is approximately 2×10^{-5} cm/sec.

ACKNOWLEDGMENTS

The author wants to thank H. Henrickson for his help in constructing the drive and F. Snively for building the power amplifier.